

Polymeric Thermal Actuation Using Laminates Based on Polymer–Clay Nanocomposites

Biqiong Chen,¹ Shuo Liu,² Julian R. G. Evans³

¹Department of Mechanical and Manufacturing Engineering, Trinity College Dublin, College Green, Dublin 2, Ireland

²Department of Materials, Queen Mary University of London, Mile End Road, London E1 4NS, United Kingdom

³Christopher Ingold Laboratories, Department of Chemistry, University College London, 20 Gordon Street, London, WC1H 0AJ, United Kingdom

Received 21 August 2007; accepted 28 January 2008

DOI 10.1002/app.28224

Published online 18 April 2008 in Wiley InterScience (www.interscience.wiley.com).

ABSTRACT: Polymer and polymer–clay nanocomposite laminates were prepared as transparent thermal actuators with possible uses in automatic aeration and ventilation or as thermal switches. Low levels of smectite clay addition reduced the thermal expansion coefficient of poly(methyl methacrylate) (PMMA) but retained optical clarity and reduced water absorption. X-ray diffraction and transmission electron microscopy were used to confirm the formation of PMMA–clay nanocomposites, and dynamic mechanical analysis was used to measure the

coefficients of thermal expansion. The experimental values of the radius of curvature of the laminates from cantilever bending tests were in good agreement with the theoretical predictions for composite bars with only 4 wt % (nominally 1.3 vol %) mineral reinforcement. © 2008 Wiley Periodicals, Inc. *J Appl Polym Sci* 109: 1480–1483, 2008

Key words: clay; composites; lamellar; nanocomposites; thermal properties; thermoplastics

INTRODUCTION

Polymer–clay nanocomposites are based on the reinforcement of polymers by high-aspect-ratio fillers derived from smectite clays. The reinforcing units have low overall dimensions and occupy such small volume fractions that conventional processing is not impeded.^{1–3} The addition of 5 wt % clay can substantially enhance mechanical and barrier properties of polymers and reduce expansion coefficients, and yet substantial translucency or even transparency can be retained.

Thermal actuators, constructed from laminated polymers with different coefficients of thermal expansion (CTEs), have been made for packaging and medical applications in which “windows” cut into the polymer film open in hot environments to allow aeration but close when the temperature falls.^{4,5} The aim of this work was to laminate nearly identical high- and low-expansion materials to avoid adhesion problems by the use of a polymer and its nanocomposite. The composite beam might be used to produce thermally actuated windows or transparent heat-sensitive switches and sensors. We report

CTEs and water absorption properties of poly(methyl methacrylate) (PMMA)–clay nanocomposites and the bending behavior of PMMA/PMMA–clay nanocomposite laminated beams as a function of temperature.

EXPERIMENTAL

PMMA with a molecular mass of 35,000 from Fisher Scientific (Loughborough, UK) and two quaternary ammonium-modified montmorillonite clays, Bentone 107 (inorganic content: 68%) and Bentone 1651 (inorganic content: 62%), which were generously provided by Elementis Specialties (Highstown, NJ), were used. PMMA–clay nanocomposites were prepared by melt processing at 170°C on a twin-roll mill. Preweighed amounts of clay were gradually added to the PMMA melt on the rolls to produce composites containing an inorganic content of 4 or 8 wt %. The mixture was stripped from the rolls and refed at least five times to ensure lateral mixing.

A Siemens D5000 X-ray diffractometer (40 kV, 40 mA) (Camberley, UK) equipped with a graphite monochromator and with Cu K α_1 radiation (wavelength = 0.15406 nm) was used for X-ray diffraction (XRD) of the composites. The aperture slits were set at 0.1°, and the scanning step was 0.02° with a scan time of 2.5 s per step. Transmission electron microscopy (TEM) was conducted on a JEOL JEM2010 electron microscope (Welwyn Garden City, UK) operated at

Correspondence to: J. R. G. Evans (j.r.g.evans@ucl.ac.uk).

Contract grant sponsor: Engineering and Physical Sciences Research Council (United Kingdom); contract grant number: GR/T24166.

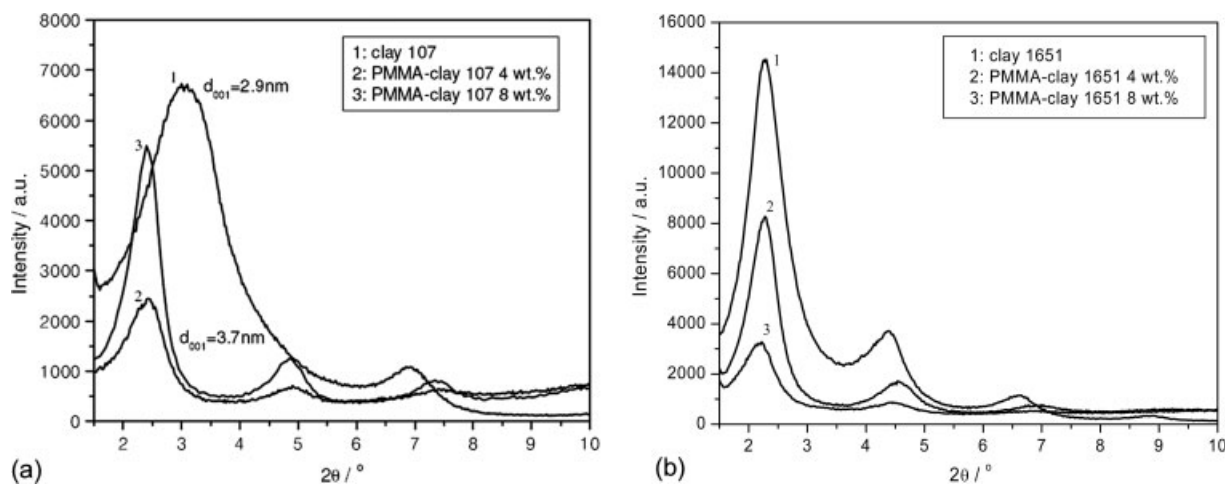


Figure 1 XRD traces of clay and PMMA–clay nanocomposites.

200 kV with Kodak SO-163 film (Hemel Hempstead, UK). TEM specimens were prepared by the ultramicrotoming of pretrimmed nanocomposite blocks with a diamond knife on a Reichert Om U2 microtome (DePew, NY) at room temperature to produce sections with a thickness of appropriately 70 nm.

CTEs were measured with a dynamic mechanical analyzer (DMA Q800, TA Instruments, Crawley, UK) with the static force set at 100 μ N. The heating rate was 3°C/min. The specimens, approximately 20 mm \times 5 mm \times 1 mm, were thermally cut from bars that were pressed at 170°C for 60 s with a hydraulic press and had a surface-polished edge. Cantilever bending tests were carried out in an oven with an observation window. One end of each specimen was encastered adjacent to a metal reference beam. A cathetometer with a resolution of 10 μ m was used to measure the deflection of the PMMA/PMMA–clay nanocomposite laminates prepared by the pressing of the two sheets together at 130°C for 300 s on a hydraulic press. The component sheets were prepared in advance by the pressing of granules at 170°C for 60 s. Water absorption measurements were conducted according to ASTM D 570. Five specimens of 50 mm \times 50 mm \times 3 mm were separately immersed in 200 mL of distilled water in beakers, which were kept at 23 \pm 1°C. The specimens were weighed 0, 0.5, 1, 2, 48, 72, and 168 h after the surface water was wiped off with a dry cloth. The average values are reported.

RESULTS AND DISCUSSION

Figure 1 shows XRD traces of clays before and after mixing with PMMA. 2θ of the (001) peak of clay 107 [Fig. 1(a)] is displaced to a lower angle after mixing, being 3.1° versus 2.4°. This corresponds to an increase in the basal plane spacing (d_{001}) of the clay

from 2.9 to 3.7 nm ($d_{002} = 1.8$ nm and $d_{003} = 1.2$ nm), which suggests intercalation of PMMA into clay galleries. Both clay addition levels give the same d_{001} value. The (001) peak of clay 1651 [Fig. 1(b)] retains its initial value at $2\theta = 2.3^\circ$ after mixing with PMMA at different ratios. d_{001} of this clay is initially large, being 3.8 nm ($d_{002} = 2.0$ nm and $d_{003} = 1.3$ nm), and it is possible that PMMA intercalates into the galleries without increasing d_{001} .⁶ As XRD is inconclusive in this case, TEM is needed to determine whether intercalation has occurred.

A TEM micrograph of the PMMA–clay 1651 nanocomposite is shown in Figure 2. Both single clay platelets and clay tactoids with several platelets (ranging from 2 to 8) stacking together can be seen in the image, suggesting both exfoliation and intercalation. If PMMA and clay 1651 form conventional composites, a large proportion of clay agglomerates

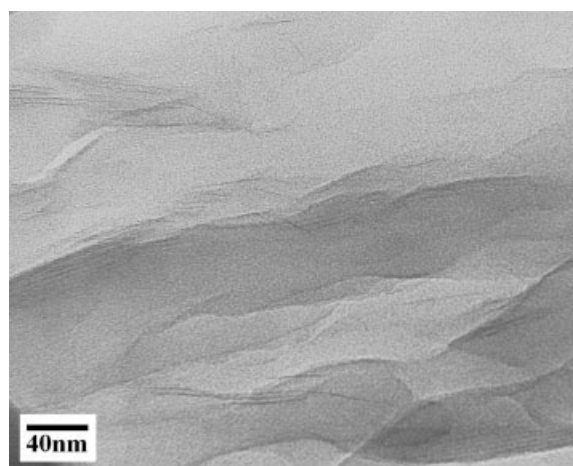


Figure 2 TEM image of the PMMA–clay 1651 nanocomposite with 4 wt % clay.

TABLE I
CTEs of PMMA and Its Nanocomposites

Specimen	CTE ($10^{-6} \text{ }^{\circ}\text{C}^{-1}$) ^a
PMMA	66
PMMA–clay 107 (4 wt %)	59
PMMA–clay 107 (8 wt %)	36
PMMA–clay 1651 (4 wt %)	54
PMMA–clay 1651 (8 wt %)	46

^a Average value between 40 and 75°C.

should be detected, but this is not seen in the image. Thus, it can be concluded that although XRD does not show an increase in d_{001} , PMMA and clay 1651 form nanocomposites rather than conventional composites.

CTEs of PMMA and PMMA–clay nanocomposites are listed in Table I. Measurements were carried out below the onset glass-transition temperature of PMMA of 112°C, as measured by differential scanning calorimetry (not shown). CTE for PMMA was measured to be $66 \times 10^{-6} \text{ }^{\circ}\text{C}^{-1}$, which is similar to the values reported in the literature, 66×10^{-6} ⁷ and $70 \times 10^{-6} \text{ }^{\circ}\text{C}^{-1}$.^{8,9} The presence of clay decreases CTE by up to 45% with the materials studied. A higher clay loading gives a lower CTE, and this can be attributed to the lower CTE for silicate platelets versus the polymer. XRD traces (Fig. 1) do not suggest better dispersion for the higher clay loading, as evidenced by the width at half-intensity of the (001) peak, so the dispersion degree is a secondary effect in PMMA–clay 107 nanocomposites. Clay 1651 at 4 wt % provides a slightly lower CTE than clay 107 at the same loading. Clay 1651 forms an intercalated–exfoliated nanocomposite with PMMA, and the nanocomposite gives a greater d_{001} value than

clay 107, which indicates better dispersion. This result may imply that better dispersion of clay platelets reduces CTE of the composite, but the data are limited. It is known that orientation has a pronounced effect on CTE because of the anisotropic shape of the reinforcing unit,¹⁰ and the compression molding and lamination steps are also likely to influence the CTE.

At room temperature, the laminates had an initial curvature toward the polymer side resulting from cooling from the heated press. With increasing temperature, the laminates returned to being horizontal. If a composite beam is initially horizontal and bends with increasing temperature, the radii of curvature for the beam can be calculated from bending geometry:

$$R_e = \frac{x^2 + \delta^2}{2\delta} \quad (1)$$

where R_e is the radius of curvature, x is the length of the beam (50 mm in this case), and δ is the deflection with respect to the reference beam. Because the deflections are small ($\delta/x < 0.11$) and simplification of eq. (1) to give $R_e = x^2/2\delta$ produces an error of less than 1%, the deformation can be expressed as that for an initially straight beam to facilitate interpretation. The results for R_e , calculated with eq. (1), are plotted in Figure 3 in comparison with the theoretical values, which are calculated as follows:¹¹

$$R_t = \frac{E_p h_p^4 + 4E_p E_n h_p^3 h_n + 6E_p E_n h_p^2 h_n^2 + 4E_p E_n h_p h_n^3 + E_n^2 h_n^4}{6E_p E_n (h_p + h_n) h_p h_n (\alpha_p - \alpha_n) \Delta T} \quad (2)$$

where R_t is the theoretical value of the radius of curvature, E is Young's modulus, α is the thermal

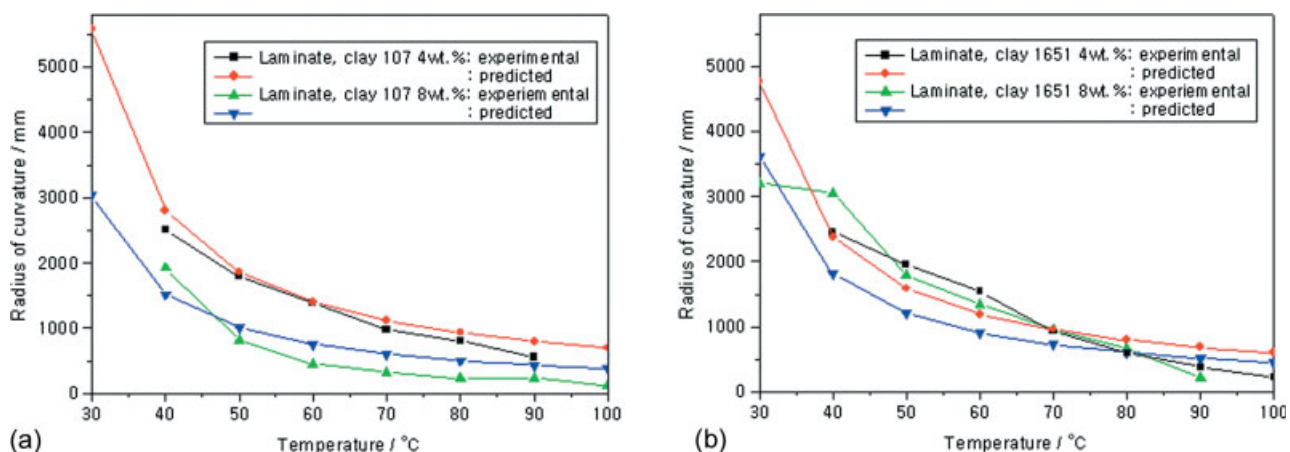


Figure 3 Radius of curvature versus the temperature for PMMA/PMMA–clay nanocomposite laminates. The experimental and theoretical values are in good agreement at 4 wt % clay [Color figure can be viewed in the online issue, which is available at www.interscience.wiley.com.]

expansion coefficient, h is the thickness of a component of the composite beam, and ΔT is the change in temperature. The subscripts p and n refer to the polymer and nanocomposite, respectively. When $E_p \approx E_n$, the equation simplifies to

$$R_t = \frac{h_p^4 + 4h_p^3h_n + 6h_p^2h_n^2 + 4h_ph_n^3 + h_n^4}{6(h_p + h_n)h_ph_n(\alpha_p - \alpha_n)\Delta T} \quad (3)$$

The E values of the nanocomposites, measured with the pulse-echo ultrasonic equipment, were within 10% of that of PMMA, and simplification of eq. (2) to give eq. (3) produced less than 0.1% error. Thus, eq. (3) was used for the calculation of the theoretical values. The thicknesses h_p and h_n were measured by a vernier caliper with samples of the laminates fractured in a way that produced delamination.

Figure 3 shows that the theoretical and experimental values of the radius of curvature are in good agreement for each composite beam, except for the laminate made with 8 wt % clay 1651. This coincidence indicates that the flexural behavior of the composite beams can generally be predicted for design purposes, provided that the CTEs are known. The problem with the 8 wt % composite made with clay 1651 was that the laminate did not join evenly, and this produced varying thicknesses of the composite layer.

Figure 4 shows that in the presence of clay, the water absorption of PMMA decreases, and this gives the nanocomposites greater stability in water than PMMA. However, the PMMA-clay nanocomposites retain considerable optical clarity (Fig. 5). The size of single clay platelets is about $50 \times 50 \times 1 \text{ nm}^3$, which is smaller than the wavelength of visible light (400–700 nm). Also, if clay platelets disperse as interca-

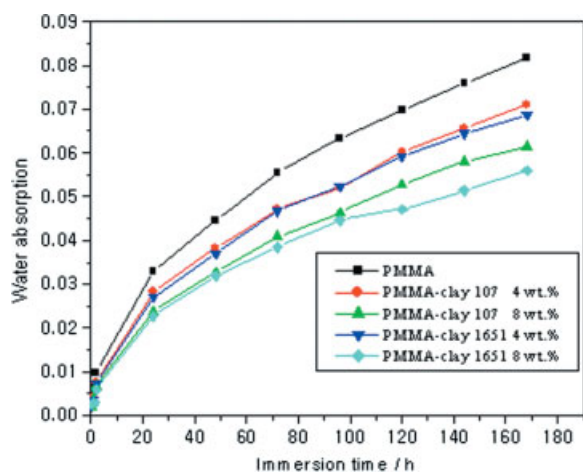


Figure 4 Water absorption curves of PMMA and PMMA-clay nanocomposites. [Color figure can be viewed in the online issue, which is available at www.interscience.wiley.com.]

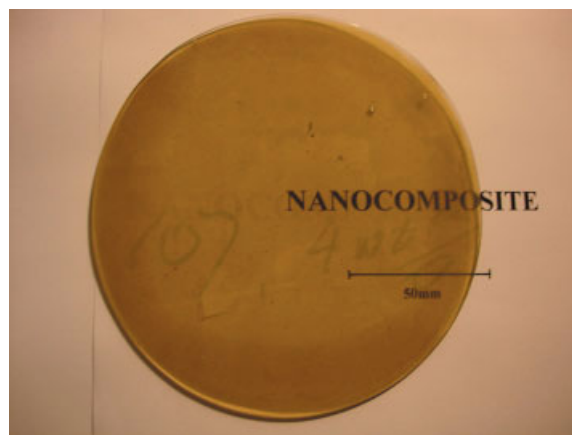


Figure 5 Photograph of the PMMA-clay 107 nanocomposite (4 wt %) tablet with a thickness of 2.5 mm. [Color figure can be viewed in the online issue, which is available at www.interscience.wiley.com.]

lated stacks, their total size is still smaller than the wavelength. For example, in Figure 2, the largest length of clay stacks is less than 150 nm.

CONCLUSIONS

We have demonstrated that potential polymeric thermal actuators can be produced with a polymer and its clay nanocomposites. PMMA-clay nanocomposites were prepared by melt processing and characterized with XRD and TEM. The CTE and water absorption of PMMA were both reduced by clay, whereas the optical clarity of PMMA was not greatly affected. The deflection of the composite beam prepared from laminates of PMMA and its clay nanocomposites behaved in the way predicted by theory except when it was not possible to obtain uniform lamination. Such laminates could be used for automatic ventilation, switches, or sensors.

References

- Pinnavaia, T. J.; Beall, G. *Polymer-Clay Nanocomposites*; Wiley: Chichester, England, 2000.
- Chen, B. *Br Ceram Trans* 2004, 103, 241.
- Chen, B.; Evans, J. R. G. *Macromolecules* 2006, 39, 1790.
- Challis, A. A. L.; Bevis, M. J. U.S. Pat. 5,672,406 (1997).
- Challis, A. A. L.; Bevis, M. J. U.S. Pat. 5,834,093 (1998).
- Zhang, J.; Jiang, D. D.; Wang, D.; Wilkie, C. A. *Polym Degrad Stab* 2006, 91, 2665.
- Igeta, M.; Banerjee, K.; Wu, G.; Hu, C.; Majumda, A. *IEEE Electron Device Lett* 2000, 21, 224.
- Lee, S.; Kim, D.; Bryant, M. D.; Ling, F. F. *Sens Actuators A* 2005, 118, 226.
- Griffiths, S. K.; Crowell, J. A. W.; Kistler, B. L.; Dryden, A. S. *J Micromech Microeng* 2004, 14, 1548.
- Okada, A.; Usuki, A. *Mater Sci Eng C* 1995, 3, 109.
- Timoshenko, S. P. *J Opt Soc Am* 1925, 11, 233.